Table IV. Bond Distances and Bond Angles for $CpW(NO)(\eta^3\text{-}C_3H_5)I$[a]

Bond Distances (Å)

W-I	2.8026 (5)	C(1)-C(2)	1.43 (1)
W-N	1.770 (5)	C(2)-C(3)	1.34 (1)
W-C(1)	2.244 (7)	N-O	1.216 (7)
W-C(2)	2.329 (8)	C(11)-C(12)	1.37 (1)
W-C(3)	2.411 (7)	C(12)-C(13)	1.35 (1)
W-C(11)	2.374 (7)	C(13)-C(14)	1.40 (1)
W-C(12)	2.324 (8)	C(14)-C(15)	1.40 (1)
W-C(13)	2.329 (8)	C(15)-C(11)	1.41 (1)
W-C(14)	2.313 (7)	C(1)-H(11)	0.7 (1)
W-C(15)	2.386 (8)	C(1)-H(12)	0.8 (1)
W-CP	2.029	C(2)-H(21)	1.0 (1)
		C(3)-H(31)	1.0 (1)
		C(3)-H(32)	0.9 (1)

Bond Angles (deg)

N-W-CP	121.7	W-N-O	172.8 (5)
I-W-CP	110.1	C(1)-C(2)-C(3)	119.0 (8)
I-W-N	89.8 (2)	W-C(1)-C(2)	75.4 (4)
I-W-C(1)	136.0 (2)	W-C(2)-C(3)	76.8 (4)
I-W-C(2)	99.9 (3)	W-C(2)-C(1)	68.4 (4)
I-W-C(3)	77.8 (2)	W-C(3)-C(2)	70.5 (5)
N-W-C(1)	90.1 (3)	C(11)-C(12)-C(13)	109.2 (9)
N-W-C(2)	87.3 (3)	C(12)-C(13)-C(14)	108.5 (8)
N-W-C(3)	110.8 (3)	C(13)-C(14)-C(15)	107.8 (8)
CP-W-C(1)	107.2	C(14)-C(15)-C(11)	106.0 (8)
CP-W-C(2)	137.2	C(15)-C(11)-C(12)	108.3 (8)
CP-W-C(3)	126.6		

[a] CP is the unweighted centroid of the ($\eta^5\text{-}C_5H_5$) ring.

Table V. ^1H and ^{13}C NMR Spectral Data for the Endo Isomer of $CpW(NO)(\eta^3\text{-}C_3H_5)I$[a]

^1H NMR Data[b]

Cp	H(11)	H(12)	H(21)	H(31)	H(32)
5.96	2.08	2.90	5.44	3.92	4.53
	$J_{11-21}=10.1$	$J_{12-21}=6.6$		$J_{31-21}=14.3$	$J_{32-21}=7.3$
	$J_{11-12}=2.6$	$J_{12-32}=3.8$		$J_{31-11}=1.8$	$J_{32-11}=1.0$
				$J_{31-32}=1.0$	

^{13}C NMR Data

Cp	C(1)	C(2)	C(3)
99.84	37.52	111.13	76.47

[a] The solvent was $CDCl_3$, and the chemical shifts (δ) are accurate to ±0.01 ppm. [b] Coupling constants are in Hz; those involving H_{21} are accurate to ±0.1 Hz, whereas the others have errors of ca. ±0.5 Hz.

AGMRX pattern for the allyl ligand contrasts with the A_2M_2X pattern displayed by the symmetric $\eta^3\text{-}C_3H_5$ group of $CpW(CO)_2(\eta^3\text{-}C_3H_5)$.[20] Assignments of resonances to individual protons have been made on the basis of coupling constants and on the assumption that the endo conformer is the principal species in solution. The indicated assignments and coupling constants (Table V) have been confirmed by a series of homonuclear decoupling experiments. The ^1H NMR spectrum also indicates the presence of another isomer of $CpW(NO)(\eta^3\text{-}C_3H_5)I$, presumably the exo conformer, but the resonances due to this isomer are not sufficiently resolved to permit detailed assignments. The observed ratio of endo:exo conformers is ca. 7:1.

The molybdenum congener, $CpMo(NO)(\eta^3\text{-}C_3H_5)I$, can be isolated in 88% yield from the reaction analogous to that represented by eq 1. Its ^{13}C and ^1H NMR spectra indicate that the allyl ligand in this complex also exhibits a significant σ–π distortion.[21] It thus appears that such distortions may well be a general feature of allyl ligands attached to metal centers having electronic asymmetry.[22]

Acknowledgment. We are grateful to the Natural Sciences and Engineering Research Council of Canada for support of this work in the form of grants to P.L. (Grant No. A5885) and J. T. (Grant No. A1121) and to the University of British Columbia Computing Centre for assistance. We also thank Professor J. W. Faller for providing us with a complete description of his results prior to publication.

Registry No. $CpW(NO)(\eta^3\text{-}C_3H_5)I$, 71341-42-9; $[CpW(NO)I_2]_2$, 71341-43-0; $Sn(C_3H_5)_4$, 7393-43-3.

Supplementary Material Available: Table III, a listing of structure amplitudes (21 pages). Ordering information is given on any current masthead page.

References and Notes

(1) Part 8: Legzdins, P.; Martin, D. T. *Inorg. Chem.* **1979**, *18*, 1250–4.
(2) Adams, R. D.; Chodosh, D. F.; Faller, J. W.; Rosan, A. M. *J. Am. Chem. Soc.* **1979**, *101*, 2570–8 and references therein.
(3) The synthesis and characterization of $[CpW(NO)I_2]_2$ will be described in a future publication.
(4) Elemental analyses were performed by Mr. P. Borda of this department.
(5) The IR spectrum was recorded on a Perkin-Elmer 457 spectrophotometer and was calibrated with the 1601-cm^{-1} band of polystyrene film.
(6) The melting point was taken in a capillary and is uncorrected.
(7) (a) Busing, W. R.; Levy, H. A. *Acta Crystallogr.* **1957**, *10*, 180–2. (b) Coppens, P.; Leiserowitz, L.; Rabinovich, D. *Ibid.* **1965**, *18*, 1035–8.
(8) (a) Becker, P. J.; Coppens, P. *Acta Crystallogr., Sect. A* **1974**, *30*, 129–47. (b) Becker, P. J.; Coppens, P. *Ibid.* **1975**, *31*, 417–25. (c) Coppens, P.; Hamilton, W. C. *Ibid.* **1970**, *26*, 71–83.
(9) Cromer, D. T.; Liberman, D. *J. Chem. Phys.* **1970**, *53*, 1891–8.
(10) Cromer, D. T.; Mann, J. B. *Acta Crystallogr., Sect. A* **1968**, *24*, 321–4.
(11) Stewart, R. F.; Davidson, E. R.; Simpson, W. T. *J. Chem. Phys.* **1965**, *42*, 3175–87.
(12) Supplementary material.
(13) Obtained at 70 eV on an Atlas CH4B spectrometer using the direct-insertion method with the assistance of Mr. J. W. Nip. The probe temperature was 140 °C.
(14) The priority sequence of the ligands is $I > \eta^5\text{-}C_5H_5 > \eta^3\text{-}C_3H_5 > NO$ if the organic groups are each considered as one ligand and if the extension of the *R,S* system to organometallic complexes with π-bonded ligands[15] is used.
(15) Stanley, K.; Baird, M. C. *J. Am. Chem. Soc.* **1975**, *97*, 6598–9 and references therein.
(16) Pauling, L. "The Nature of the Chemical Bond", 3rd ed.; Cornell University Press: Ithaca, N.Y., 1960; pp 232–9.
(17) The estimated standard deviations for the H(11) and H(12) distances and angles are far too high for any conclusions to be drawn regarding their being positioned in a pseudotetrahedral fashion (bent back away from the W atom) around C(1).
(18) ^1H FT NMR spectra were recorded at 270 MHz and ambient temperature by Mrs. M. M. Tracey on a departmental spectrometer employing an Oxford Instruments superconducting magnet and Nicolet Instrument Corp. hardware. ^{13}C NMR spectra were recorded on a Varian Associates CFT20 spectrometer. The indicated chemical shifts are downfield from Me_4Si.
(19) Mann, B. E. *Adv. Organomet. Chem.* **1974**, *12*, 135–213.
(20) Faller, J. W.; Chen, C. C.; Mattina, M. J.; Jakubowski, A. *J. Organomet. Chem.* **1973**, *52*, 361–86.
(21) After completion of this work, we learned from Professor J. W. Faller that he and his co-workers have fully characterized the series of complexes $CpMo(NO)(\eta^3\text{-allyl})X$ (X = NCO, CN or I; allyl = C_3H_5 or C_4H_7), all of which contain a distorted η^3-allyl ligand.
(22) ^1H NMR spectra similar to, but less fully resolved than, that depicted in Figure 2 have recently been reported for the complexes $CpMo(\eta^3\text{-allyl ester})(CO)(PPh_3)$ (Collin, J.; Charrier, C.; Pouet, M. J.; Cadiot, P.; Roustan, J. L. *J. Organomet. Chem.* **1979**, *168*, 321–36).

Contribution from the Department of Chemistry, University of South Carolina, Columbia, South Carolina 29208

Determination of the Barrier to Rotation about the Iron–Ligand Bond in Cationic $(\eta^5\text{-}C_5H_5)Fe(CO)(L)$ (L = PPh_3, $P(OPh)_3$) π-Alkyne and π-Alkene Complexes

D. L. Reger* and C. J. Coleman

Received January 5, 1979

In 1964 Cramer reported the first detailed dynamic NMR study of rotation of alkenes about the bond axis from a transition metal to the midpoint of the carbon–carbon double bond.[1] Since that time, many similar processes have been studied and the activation energies or the so-called barriers

Table I. Energies of Activation

complex	$\Delta G^{\ddagger}$, kcal/mol	T, °C	method of determn[a]
$[(\eta^5\text{-}C_5H_5)Fe(CO)[P(OPh)_3](\eta^2\text{-}3\text{-hexyne})]BF_4$	13.1	+25	I
	13.2	−23	II
$[(\eta^5\text{-}C_5H_5)Fe(CO)[P(OPh)_3](\eta^2\text{-diphenylacetylene})]BF_4$	13.9	−5	II
$[(\eta^5\text{-}C_5H_5)Fe(CO)[P(OPh)_3](\eta^2\text{-ethylene})]BF_4$	8.0	−95	III
$[(\eta^5\text{-}C_5H_5)Fe(CO)(PPh_3)(\eta^2\text{-}3\text{-hexyne})]BF_4$	15.0	+18	II
$[(\eta^5\text{-}C_5H_5)Fe(CO)(PPh_3)(\eta^2\text{-}2\text{-butyne})]BF_4$	14.3	+1	II
$[(\eta^5\text{-}C_5H_5)Fe(CO)(PPh_3)(\eta^2\text{-ethylene})]BF_4$	10.0	−40	III

[a] I, computer simulation; II, line broadening measurements before coalescense; III, line broadening measurements after coalescence.

to rotation of these processes have been calculated by using classical kinetic theory. Analogous complexes of η^2-alkyne ligands should also show similar behavior. Dynamic behavior for the complexes [Os(CO)(NO)(phosphine ligand)$_2$(alkyne)]PF_6[2] and $(\eta^5\text{-}C_5H_5)Cr(CO)(NO)(C_2H_2)$[3] has been observed although a dissociative mechanism could not be ruled out. More recently, a number of 16-electron η^2-alkyne complexes such as $[(\eta^5\text{-}C_5H_5)Mo[P(OMe)_3]_2(MeC_2Me)]BF_4$ have been reported to show dynamic behavior of the alkyne ligand.[4] Coupling between a phosphine ligand and the alkyne ligand in the averaged high-temperature spectrum has been observed in certain cases, ruling out a dissociative process.[4a]

In two earlier papers, we have described the synthesis and characterization of a variety of alkene and alkyne complexes of the formula $[(\eta^5\text{-}C_5H_5)Fe(CO)(L)(\eta^2\text{-ligand})]BF_4$ (L = PPh_3, $P(OPh)_3$).[5,6] These complexes with ethylene or a symmetrical alkyne as the η^2-ligand show averaged NMR spectra at room temperature, but these spectra collapse to the limiting static spectra at low temperature. Reported here is the determination of the barriers to rotation in these complexes.

Experimental Section

^{1}H NMR Spectra. The ^{1}H NMR spectra were recorded at 90 MHz on a Perkin-Elmer R-32 spectrometer equipped with variable-temperature accessory. Samples were prepared under inert atmosphere by using as solvent acetone-d_6 which had been degassed by four consecutive freeze–pump–thaw cycles. All spectra were run in the field lock mode with Me_4Si added to the sample for locking purposes. Temperature determinations were made by measuring the chemical shifts of methanol[7] at expanded sweep width (300 Hz) before and after each spectrum. The methanol was contained in a capillary drawn to a diameter of ca. 0.3 mm and this capillary centered in the tube of the sample being investigated with Teflon spacers. A trace of concentrated aqueous hydrochloric acid was added to the methanol to produce sharp singlets to aid in chemical shift determinations. All spectra of $[(\eta^5\text{-}C_5H_5)Fe(CO)[P(OPh)_3](\eta^2\text{-}3\text{-hexyne})]BF_4$ were recorded at expanded sweep width (100 Hz) and several spectra were recorded at each temperature. Spectra were recorded at ca. 10° intervals from +35 to −75 °C, except when within a 20 °C range of the coalescence temperature, in which case spectra were recorded every 3–4 °C.

Spectral Simulations. The simulated spectra were calculated by using the DNMR 3[8] computer program which had been modified by Dr. T. F. Moore to execute on the University of South Carolina's IBM-370 computer and which had been converted to double precision. The methylene resonance of $[(\eta^5\text{-}C_5H_5)Fe(CO)[P(OPh)_3](\eta^2\text{-}3\text{-hexyne})]BF_4$ was a poorly resolved multiplet and was not suitable for simulation. This complexity is expected because even in the averaged spectrum the methylene hydrogen atoms are rendered diastereotopic by the chiral metal center. The methyl resonance, in contrast, was well resolved at both high and low temperatures and was used for the simulation. The spectra were calculated by using an $AX_2 \rightleftharpoons BX_2$ spin system with nonmutual exchange. The parameters that were read into the program were the chemical shifts in hertz relative to an arbitrary reference (δ(A) = 142.0 Hz, δ(B) = 160.8 Hz, δ(X) = 53.0 Hz), the coupling constants in hertz (7.2 Hz), the effective transverse relaxation time T_2 (0.155 s) which is calculated from the line width at half-height $\Delta\nu_{1/2}$ (in Hertz) by $T_2 = 1/\pi\Delta\nu_{1/2}$, and various rate constants in inverse seconds. The calculated spectra were plotted on a CALCOMP plotter. The experimental and simulated spectra were matched by visual comparison of the spectra. The Eyring plot of ln (k/T) vs. $1/T$ was made on a Hewlett-Packard 9810A calculator using a standard least-squares analysis. The slope and Y intercept of the line were obtained directly from this analysis.

^{13}C NMR Spectra. The energies of activation obtained from initial line broadening relationships were all obtained by using ^{13}C NMR spectroscopy. Spectra were recorded on a Varian CFT-20 spectrometer equipped with variable-temperature controller. The samples were prepared under inert atomsphere by using as solvent either CH_2Cl_2 or $CHCl_3$ which had been freeze–thaw degassed immediately before use. Temperature determinations were made with a copper–constantan thermocouple before and after each run and were constant to ±1 °C. Samples were allowed to equilibrate in the probe for at least 30 min before data acquisition was initiated.

Spectra obtained during the search for the initial line broadening were run under conditions (0.5 s acquisition time and no pulse delay) which gave adequate spectra in ca. 2 h. Once the temperature corresponding to the desired line broadening was determined, a fresh sample was prepared and another spectrum obtained under conditions (1.0 s acquisition time, 1000 Hz filter bandwidth, 2000 Hz sweep width, 90° pulse flip angle, and no pulse delay) which provided the resolution needed to make accurate determinations of the line widths. Spectra with a good signal to noise ratio were then obtained after ca. 15000 scans. Generally, the line widths of the exchange-broadened lines were nearly double that of the nonbroadened lines. The slow-exchange spectra and the fast-exchange spectra were obtained ca. 30° from the exchange-broadened spectra. All spectra were recorded at expanded sweep width (80 Hz), and the line widths (in Hz) are believed to be accurate to ±0.5 Hz. A signal not affected by the exchange process, the η^5-C_5H_5 resonance, for example, was also recorded to serve as a homogeneity check.

Results and Discussion

As shown in Table I, the barrier to rotation for the ethylene and a number of alkyne derivatives of $[(\eta^5\text{-}C_5H_5)Fe(CO)(L)(\eta^2\text{-ligand})]BF_4$ (L = PPh_3, $P(OPh)_3$) has been determined by dynamic NMR methods. Taking into account error inherent in these determinations, we believe the $\Delta G^{\ddagger}$ values are accurate within ±0.5 kcal/mol. Three basic methods were used to determine the values in Table I. The first value listed for $[(\eta^5\text{-}C_5H_5)Fe(CO)[P(OPh)_3](\eta^2\text{-}3\text{-hexyne})]BF_4$ was calculated from a complete line-shape analysis. The methyl groups show as one triplet in the ^{1}H NMR spectrum at room temperature, collapsing to a pair of triplets at −38 °C. The observed and computer-simulated spectra are shown in Figure 1. From a standard Eyring plot, $\Delta H^{\ddagger}$ was calculated as 12.7 ± 0.4 kcal/mol and $\Delta S^{\ddagger}$ as −1.3 ± 1.0 eu. The value of log A (A = frequency factor) was 12.9 and the value of E_a was 13.3 ± 0.4 kcal/mol. The second barrier listed for this complex and those of the other alkyne complexes were determined by the method of initial line broadening of the static low-temperature spectra. In all cases, ^{13}C NMR spectroscopy was used in these determinations. It should be noted as an internal check that the value of $\Delta G^{\ddagger}$ determined by the complete line-shape analysis is essentially identical with that determined by the line broadening techniques. Because the ethylene complexes had lower barriers and a limiting low-temperature spectrum could not be obtained, the method[9] of line broadening after coalescence was used. In this determination, the separation of the resonances in the static spectrum was taken as 64 Hz for both complexes. This is the separation of the ethylene

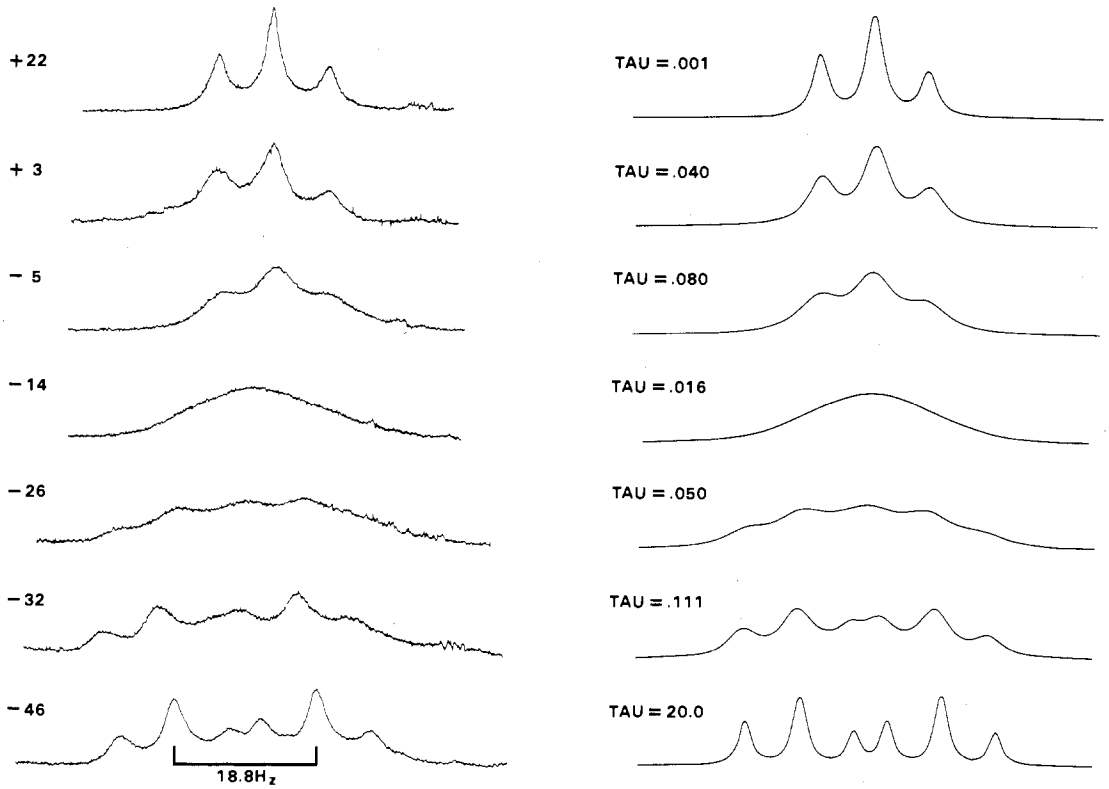

Figure 1. Observed (left) and calculated (right) ^1H NMR spectra of the methyl resonances of $[(\eta^5\text{-}C_5H_5)Fe(CO)[P(OPh)_3](3\text{-hexyne})]BF_4$ at various temperatures (°C) and lifetimes (s), respectively.

carbon resonances at −85 °C for the triphenylphosphine complex, a spectrum that was close to the static spectrum. As shown by others, a fairly large error in the determination of this number does not substantially change $\Delta G^{\ddagger}$.[10]

That we are actually observing a barrier to rotation in these complexes and not a dissociative process was shown by the observation of P–C coupling in the high-temperature spectra of all of the complexes studied for the triphenyl phosphite system. In the triphenylphosphine system, this coupling was observed only for the allene complex,[5] a complex also undergoing rotation for which the barrier could not be determined. Also, the methylene hydrogen atoms for the 3-hexyne compound are quite complex in the room-temperature averaged spectrum as would be expected for these diastereotopic atoms averaging by a nondissociative mechanism. Although P–C coupling could not be observed in the averaged spectra for the other alkyne–triphenylphosphine complexes because of thermal decomposition problems, a common mechanism is reasonable.

The barrier to rotation in these complexes consists of both a steric and an electronic component.[11] The steric factor arises when the ligand sweeps from its lowest energy position, presumably approximately parallel to the bulky $\eta^5\text{-}C_5H_5$ ring, past the other ligands. The electronic factor arises from the nonequivalence of the metal orbitals in the molecular environment causing the strength of the π-back-bonding component of the bond to vary from one configuration to another. Recent calculations on similar molecules have shown that the π-back-bonding interaction is greatest when the alkyne is parallel to the $\eta^5\text{-}C_5H_5$ ring.[12] A ground-state configuration similar to this is assumed for the molecules discussed here.

It is not possible from the data presented here to separate the electronic and steric factors because one would predict a higher barrier from both factors for the triphenylphosphine complexes. Sterically triphenylphosphine is clearly much more bulky. Electronically it is a stronger base and weaker π-back-bonding ligand than triphenyl phosphite, leaving more electron density on the metal for π back-bonding with the alkyne or ethylene ligand. That steric factors do not dominate the magnitude of these barriers is shown by comparing the diphenylacetylene and 3-hexyne complexes in the phosphite system. The barrier is only 0.8 kcal/mol higher for the diphenylacetylene complex and one would expect a much larger difference for this bulky ligand if steric factors were paramount.

The most important comparison to be made in this work is the difference in barriers between alkene and the alkyne ligands in general. Unfortunately, the acetylene complex could not be prepared. Comparison of the ethylene barriers with those of the 2-butyne and 3-hexyne complexes shows that alkynes generally can be expected to have a higher barrier to rotation than alkenes. A higher barrier for acetylene vs. ethylene in $[Os(CO)(NO)(PPh_3)_2(\eta^2\text{-ligand})]PF_6$ complexes of 2.0 kcal/mol has been reported.[2,13] A larger difference of ca. 5 kcal/mol is observed for the complexes reported here. In comparison of the results from the triphenylphosphine and triphenyl phosphite complexes with the same η^2-ligand, the phosphine complexes have a larger barrier by 2 kcal/mol. This difference presumably arises from a greater electron density at the metal for the phosphine complexes increasing the strength of the π-back-bonding interaction.

Acknowledgment. Acknowledgment is made to the donors of the Petroleum Research Fund, administered by the American Chemical Society, for the support of this project. We also thank Dr. Thomas Moore and Dr. William Dawson for assistance with the program used to simulate NMR spectra.

Registry No. $[(\eta^5\text{-}C_5H_5)Fe(CO)[P(OPh)_3](\eta^2\text{-}3\text{-hexyne})]BF_4$, 71341-56-5; $[(\eta^5\text{-}C_5H_5)Fe(CO)[P(OPh)_3](\eta^2\text{-diphenylacetylene})]BF_4$, 71341-58-7; $[(\eta^5\text{-}C_5H_5)Fe(CO)[P(OPh)_3](\eta^2\text{-ethane})]BF_4$, 71341-60-1; $[(\eta^5\text{-}C_5H_5)Fe(CO)(PPh_3)(\eta^3\text{-}3\text{-hexyne})]BF_4$, 70568-97-7; $[(\eta^5\text{-}C_5H_5)Fe(CO)(PPh_3)(\eta^2\text{-}2\text{-butyne})]BF_4$, 70568-99-9; $[(\eta^5\text{-}C_5H_5)Fe(CO)(PPh_3)(\eta^2\text{-ethene})]BF_4$, 41560-74-1.

References and Notes

(1) R. Cramer, *J. Am. Chem. Soc.*, **86**, 217 (1964).

(2) J. A. Segal and B. F. G. Johnson, *J. Chem. Soc., Dalton Trans.*, 1990 (1975).
(3) M. Herberhold, H. Alt, and C. G. Kreiter, *J. Organomet. Chem.*, **42**, 413 (1972).
(4) (a) M. Bottrill and M. Green, *J. Am. Chem. Soc.*, **99**, 5795 (1977); (b) M. L. H. Green, J. Knight, and J. A. Segal, *J. Chem. Soc., Dalton Trans.*, 2189 (1977); (c) H. G. Alt and W. Stadler, *Z. Naturforsch., B*, **32**, 144 (1977); (d) J. L. Davidson, M. Green, F. G. A. Stone, and A. J. Welch, *J. Chem. Soc., Dalton Trans.*, 738 (1976); (e) H. G. Alt, *J. Organomet. Chem.*, **127**, 349 (1977).
(5) D. L. Reger, C. J. Coleman, and P. J. McElligott, *J. Organomet. Chem.*, **171**, 73 (1979).
(6) D. L. Reger and C. J. Coleman, *Inorg. Chem.*, **18**, 3155 (1979).
(7) A. C. Van Gett, *Anal. Chem.*, **42**, 679 (1970).
(8) D. A. Kleier and G. Binsch, Program 165, Quantum Chemistry Program Exchange, Indiana University, Bloomington, Ind.
(9) J. W. Faller in "Advances in Organometallic Chemistry", Vol. 16, F. G. A. Stone and Robert West, Eds., Academic Press, New York, 1977, p 213.
(10) J. W. Faller and B. V. Johnson, *J. Organomet. Chem.*, **88**, 101 (1975).
(11) F. A. Cotton in "Dynamic Nuclear Magnetic Resonance", L. M. Jackman and F. A. Cotton, Eds. Academic Press, New York, 1975, p 337.
(12) B. E. R. Schilling, R. Hoffmann, and D. L. Lichtenberger, *J. Am. Chem. Soc.*, **101**, 585 (1979).
(13) J. A. Segal and B. F. G. Johnson, *J. Chem. Soc., Dalton Trans.*, 677 (1975).

Contribution from the Department of Chemistry, University of Arkansas, Fayetteville, Arkansas 72701

Photochemical Linkage Isomerization in Coordinated SO_2[1]

D. A. Johnson* and V. C. Dew

Received May 22, 1979

Sulfur dioxide (SO_2) is an extremely versatile ligand forming a variety of complexes, usually with low oxidation state metal ions.[2] The structural chemistry of complexes involving a direct metal–sulfur dioxide interaction is quite interesting with a number of well-established examples of the planar sulfur-bonded (i), pyramidal sulfur-bonded (ii), and η^2 (iii) structures shown below. Examples of oxygen-to-metal SO_2 coordination (iv) are not known for transition metals; however, this mode of coordination has been observed for the Lewis acid SbF_5.[3]

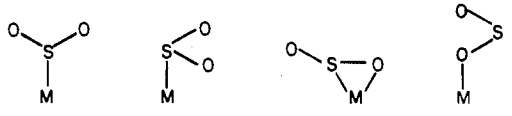

i ii iii iv

An analogy has been drawn between the metal–ligand stereochemical behavior of nitric oxide (NO) and sulfur dioxide (SO_2), and the importance of the energy match between the π^* molecular orbitals of these ligands and the nd orbitals of the metal ion in determining the stereochemistry of the interaction has been emphasized.[4,5] In this formalism, structures i and ii can be considered analogues of linear and bent nitrosyl ligands, respectively. In addition to the electronic relationship between NO and SO_2 noted above, sulfur dioxide is formally isoelectronic with NO_2^- and the isomeric interactions comparable to i, iii, and iv have identified or postulated[6,7] analogues in the chemistry of the nitrite ligand. Thus, the stereochemistry of transition metal–SO_2 interactions is a mixture of parallels to the behavior of the ligands NO and NO_2^-.

Despite the many interaction modes for ligating SO_2, linkage isomers have not been observed.[8] We wish to report a previously undetected example of *photochemically induced* linkage isomerism in the solid-state photolysis of $[Ru(NH_3)_4Cl(SO_2)]Cl$ at 365 nm. The unstable linkage isomers of the SO_2 ligand produced in this photolysis can be trapped at low temperatures (25–195 K). The isomeric composition of the photoproduct can be altered by variation of the temperature of trapping and photolysis time, and infrared and electronic spectra indicate that more than one photoproduct is obtained in long photolyses at 25 K.

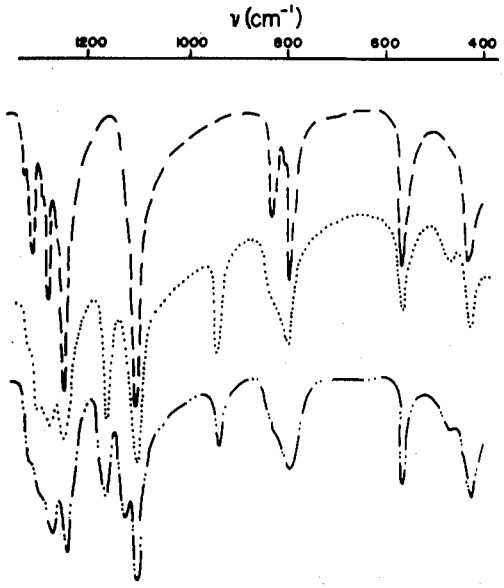

Figure 1. Infrared spectra of $[Ru(NH_3)_4Cl(SO_2)]Cl$ in the 1400–400-cm^{-1} region. From top to bottom these spectra are for the starting complex at 25 K, a sample photolyzed at 195 K, and a 25 K photolysis, respectively. Both photolyses are at 365 nm.

Experimental Section

The complex $[Ru(NH_3)_4Cl(SO_2)]Cl$ was prepared by the method of Wiberley et al.[9] Partial exchange of the sulfur dioxide oxygens was accomplished by dissolving the starting material in $H_2{}^{18}O$–$H_2{}^{16}O$ solution (pH > 3) which leads to hydration of the SO_2 to coordinated SO_3H^-.[10] The ^{18}O exchanged product was precipitated by bubbling with HCl (gas).

Infrared and electronic spectra were obtained in pressed KBr pellets (IR, UV–vis) and frozen HCl–H_2O glasses (visible) by using Perkin-Elmer 457 and Cary 14 spectrometers, respectively. Low-temperature spectra were measured by using a single-temperature cryostat of standard design and a variable-temperature Cryogenic Technology, Inc., Cryocooler.

Results

The starting complex has ν(SO) 1255 and 1110 cm^{-1} corresponding to the asymmetric and symmetric S–O stretching modes, respectively.[9] Photolysis of a KBr pellet of this complex at 195 K with 365-nm radiation causes a decrease in these bands and the production of new sulfur–oxygen absorptions at ν_I(SO) 1165 and ν_{II}(SO) 940 cm^{-1} (see Figure 1). The identification of these bands as ν(SO) is supported by preparation and photolysis of the deuterated and partially ^{18}O-exchanged samples of the starting material. Comparable infrared changes are observed for KBr pellets and Nujol mulls indicating that the photoreaction does not involve substitution by the matrix Br^- ions. The direction of the shifts in ν(SO) argues against formation of free SO_2, and the apparently low activation energy for the thermal reverse process suggests that substitution of the ammine ligands by lattice halide is unlikely. The infrared shifts suggest the photochemical conversion of the planar Ru(II)–SO_2 linkage of the starting material to either isomer ii or iii. The observed infrared changes are completely reversible at room temperature. Of the two suggested structures, the difference between the ν_I(SO) and ν_{II}(SO) (225 cm^{-1}) for the photoisomer is most consistent with the η^2 structure (iii). The infrared spectrum of the photolysis product of a partially ^{18}O-exchanged sample of $[Ru(NH_3)_4$-

0020-1669/79/1318-3273$01.00/0